Residual-Stress Distributions Produced by Strain-Gage Surface Preparation

by Paul S. Prevey

ABSTRACT—Abrasion of a metallic surface to improve bonding during strain-gage installation is generally thought to produce negligible effect on the measurement of residual stresses by blind hole drilling. However, residual stresses induced by surface abrasion may affect residual-stress measurements in shallow subsurface layers of residual-stress fields produced by processes such as grinding and shot peening.

The residual-stress and cold-work distributions produced by four methods of abrasive surface preparation and etching were studied by X-ray diffraction in fully annealed AISI 1018 steel. The surface residual stresses produced by abrasion ranged from tension to compression with magnitudes as high as 80 percent of the yield strength. Cold work was induced to depths of 20 to 60 μm. Etching produced low magnitude surface stresses and negligible cold work.

Introduction

Accurate measurement of any physical property requires that the instrumentation and technique used have a minimum effect upon the property measured. The blind-hole-drilling method for residual-stress measurement, which was originally developed assuming a uniform stress field throughout the depth of the hole, has been refined to allow the determination of the residual-stress distributions as a function of depth by incremental drilling.[2,3] Incremental drilling increases the depth resolution of the method to measure residual-stress distributions near the surface of the specimen produced by such processes as machining, grinding, or shot peening.

During phase one of a round-robin study sponsored by the SEM Residual Stress Measurement Committee,[4] the residual stresses near the surface of a nominally stress-free AISI 1018 steel specimen were measured by both X-ray diffraction and blind-hole-drilling methods. Preparation of the sample for strain-gage bonding was found to

produce significant residual stress at the sample surface. The residual-stress distribution produced by one of the hole-drilling participants, measured by X-ray diffraction after removing the strain-gage rosette with an organic solvent, is shown in Fig. 1. The shallow, highly compressive residual-stress distribution is attributed to the abrasion of the sample surface, a common practice to improve strain-gage bonding.

Abrasion of the sample surface for strain-gage installation could result in several potentially significant sources of experimental error. First, the residual-stress field induced by abrasion could alter shallow subsurface layers of residual-stress fields to be measured. This could be especially important for fields of a depth comparable to the residual stresses caused by abrasion. Second, the induced residual stress, which may vary in magnitude and sign with direction, could result in local yielding beneath the strain-gage grids during measurement.

To characterize the residual-stress distributions produced by surface preparation, five locations were prepared on a 1018 steel coupon, using four abrasive procedures and etching. The principal subsurface residual-stress distributions and the depth of the cold-worked layer were determined for each surface-preparation technique.

Sample Preparation

A single sample of AISI 1018 steel, originally prepared as part of the SEM Residual Stress Measurement Committee round robin, was used in this investigation. The sample had nominal dimensions of 14.7 $\times$ 1.2 $\times$ 2.5 cm, and had received a complex annealing heat treatment intended to produce an essentially residual stress-free specimen.[4] The resulting specimen had a hardness of nominally 60 HRB and a yield strength on the order of 300 MPa in the fully annealed condition.[5]

Five 2.5-cm areas were prepared on the 14.7 $\times$ 1.2-cm face of the specimen. Four areas were prepared by various mechanical lapping and sanding techniques typical of those recommended by strain-gage manufacturers and in the literature. Abrasion was in the direction perpendicular to the longitudinal axis of the specimen. Sufficient material was removed by each method to ensure that the resulting

Paul S. Prevey (SEM Member) is President, Lambda Research Inc., 1111 Harrison Avenue, Cincinnati, OH 45214-1801.

residual-stress distributions would be due solely to the method of preparation. Location No. 4 was prepared by etching the surface for ten minutes with a 10-percent nitric acid-methanol solution (nital). The method of surface preparation, and the amount of material removed, are summarized in Table 1. Locations 2 and 3 were also treated with chemical cleaning agents.

Experimental Technique

At each of the five locations, X-ray diffraction residual-stress measurements were made in the directions parallel, 45 degrees, and perpendicular to the longitudinal axis of the sample at the surface and at nominal depths of 5, 10, 20, 30, 40, 50, 60, 100, and 150 μm. The two-inclined angle technique[6] was used, employing the diffraction of chromium $K\alpha$ radiation from the (211) planes of the BCC structure of the AISI 1018 steel. The (211) diffraction peak angular position at each of the ψ tilts employed for measurement was determined from the position of the $K\alpha_1$ diffraction peak separated from the superimposed $K\alpha$ doublet, assuming the diffraction peak profile to be described by a Pearson VII distribution function in the high back-reflection region.[7] The diffracted intensity, peak breadth, and position of the $K\alpha_1$ diffraction peak were determined by fitting a Pearson VII function profile by nonlinear least-squares regression after correction for the Lorentz-polarization and absorption effects, and for a linearly sloping background intensity.

Macrostress Distribution

The X-ray diffraction measurements were made on a GE horizontal diffractometer modified for residual-stress measurement using a Bragg-Brentano focusing geometry. Details of the diffractometer technique are outlined below.

$$\text{Incident-beam divergence} = 3.0 \text{ deg}$$
$$\text{Detector} = \text{sodium iodide scintillation}$$
$$\psi \text{ rotation} = 0.0\text{-}45.0 \text{ deg}$$
$$\text{Counts per point} = 200,000$$
$$\tfrac{1}{2} S_2 = 5.84 \pm 0.07 \times 10^{-6}$$
$$\text{Irradiated area} = 8 \times 8 \text{ mm}$$

The value of the X-ray elastic constant, $\tfrac{1}{2} S_2$, for the crystallographic direction normal to the (211) planes of AISI 1027 steel was determined empirically by loading a simple rectangular beam manufactured from AISI 1027 steel in four-point bending on the diffractometer to known stress levels, and measuring resulting strain in the (211) direction.[8] The macroscopic residual stress was calculated from the lattice strain measured in the (211) crystallographic direction using $\tfrac{1}{2} S_2$ for AISI 1027 steel. The X-ray elastic constants were not determined for AISI 1018 steel.

The specimen exhibited a relatively coarse grain size. Residual-stress measurements were performed with the specimen rocking ± 2.5 deg to minimize the influence of the coarse grain size on the location of the diffraction peak position.

Material was removed for subsurface measurement by electropolishing in a sulfuric-phosphoric-acid electrolyte, minimizing possible alteration of the subsurface residual-stress distribution. The (211) lattice spacing, measured as a function of depth, was corrected for the effects of penetration of the radiation into the subsurface stress

TABLE 1—SURFACE PREPARATION

Location	Preparation Method	Amount Removed (μm)	Reference
(1)	400-grit dry power-disk sanded	76.	1, 3, 5
(2)	220-grit wet hand lap, plus conditioner A and neutralizer	50.	1, 2, 4, 5
(3)	400-grit wet hand lap, plus conditioner A and neutralizer	25.	2, 4
(4)	Nital etch (10-minute exposure)	13.	
(5)	120-grit dry power-belt sanded	160.	

(1) Micromeasurements Instruction Bulletin B-129 (May 1976)
(2) Micromeasurements Instruction Bulletin B-137-10 (1979)
(3) BLH Electronics Product Data Sheet 109 (1975)
(4) W.T. Bean, Inc. Instruction Bulletin, Sheet 6 (1963)
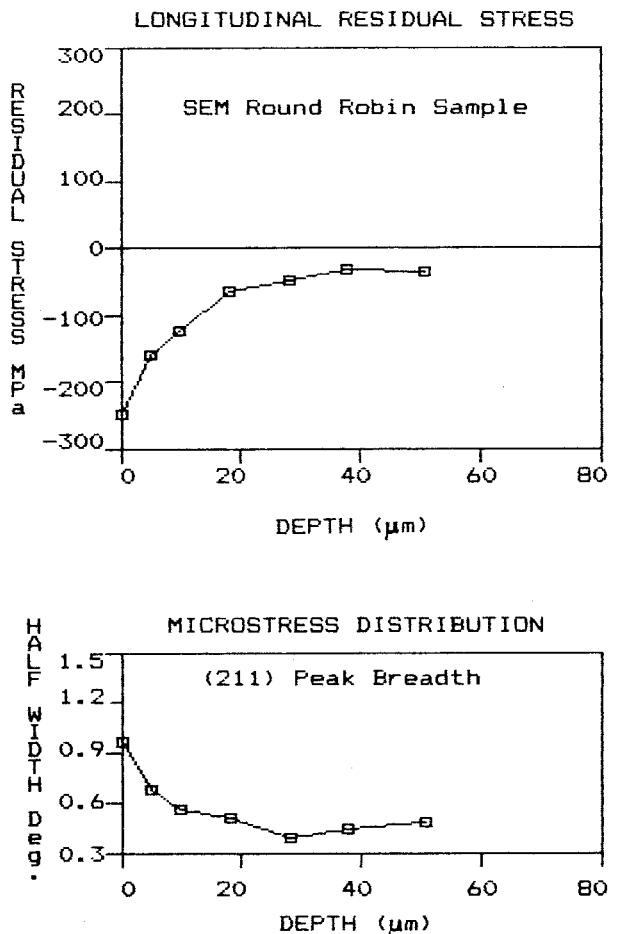(5) C.C. Perry and H.R. Lissner, THE STRAIN GAGE PRIMER, 2nd Ed., McGraw-Hill, 33-36 (1962)

Fig. 1—Longitudinal residual-stress and (211) peak-breadth distributions produced by strain-gage installation on a 1018 steel SEM round-robin sample

gradient.[9] The macroscopic residual-stress distributions were further corrected for stress relaxation caused by layer removal using a closed-form solution developed for a rectangular beam.[10]

The residual-stress distributions in the directions parallel, 45 degrees, and perpendicular to the axis of the specimen, determined at each depth and location, were combined using Mohr's circle for stress to determine the maximum and minimum normal stress with respect to the longitudinal axis of the sample.

The magnitude of the systematic instrumental error caused by diffractometer misalignment, beam divergence and displacement of the diffracting volume was monitored using a powdered-iron zero-stress standard in accordance with ASTM specification E915-83,[11] and was found to be −2 MPa. Random error due to counting statistics and sample positioning was on the order of ±14 MPa.

Although the results presented here were obtained by the two-angle technique, several measurements were made by the $\sin^2 \psi$ technique,[13] employing six positive ψ tilts, ranging from 0 to 45 degrees. With the specimen rocking during measurement, the results showed excellent linearity of the lattice spacing of the (211) planes as a function of $\sin^2 \psi$, indicating a plane-stress residual-stress field and a standard deviation of ±8 MPa.

Microstress Distribution

The (211) diffraction peak breadth at half height was calculated as a function of depth from the width of the Pearson VII distribution function fitted to the (211) $K\alpha_1$ diffraction peak profile. The peak breadth increases as the coherent diffracting domain size decreases and as lattice microstrain, caused by dislocations and point defects, increases. The depth at which the (211) peak breadth approaches the value for the annealed subsurface material is assumed to be the depth of significant cold work and disruption of the crystal lattice.

No empirical relationship was developed relating the (211) diffraction-peak breadth and known amounts of cold work for 1018 steel. Previous investigations for the nickel-base alloys, Inconel 600,[12] Rene 95, and Inconel 718, have shown that the (420) peak breadth increases approximately linearly with the amount of cold work. Abrasive polishing has been shown to induce 20-percent cold work at the surface of Inconel 600.

Results and Discussion

The macroscopic and microscopic residual-stress distributions are presented in Figs. 1-6. Compressive stresses are shown as negative values. Figure 1 shows the residual-stress distribution for the round-robin specimen in the area prepared for strain gaging by one of the hole-drilling participants. Measurements were made on this specimen only in the direction parallel to the longitudinal axis of the specimen.

Figures 2-6 show the results for the test areas on the AISI 1018 steel specimen prepared as shown in Table 1. The minimum and maximum normal residual stresses were calculated from measurements made in the directions parallel, 45 degrees, and perpendicular to the axis of the sample. The orientation of the maximum stress is given by the angle ϕ, taken to be a positive angle counterclockwise from the longitudinal direction. The microstress distribution is presented in terms of the (211) diffraction peak breadth. The plots of ϕ as a function of depth have been connected for clarity by straight lines between the depths
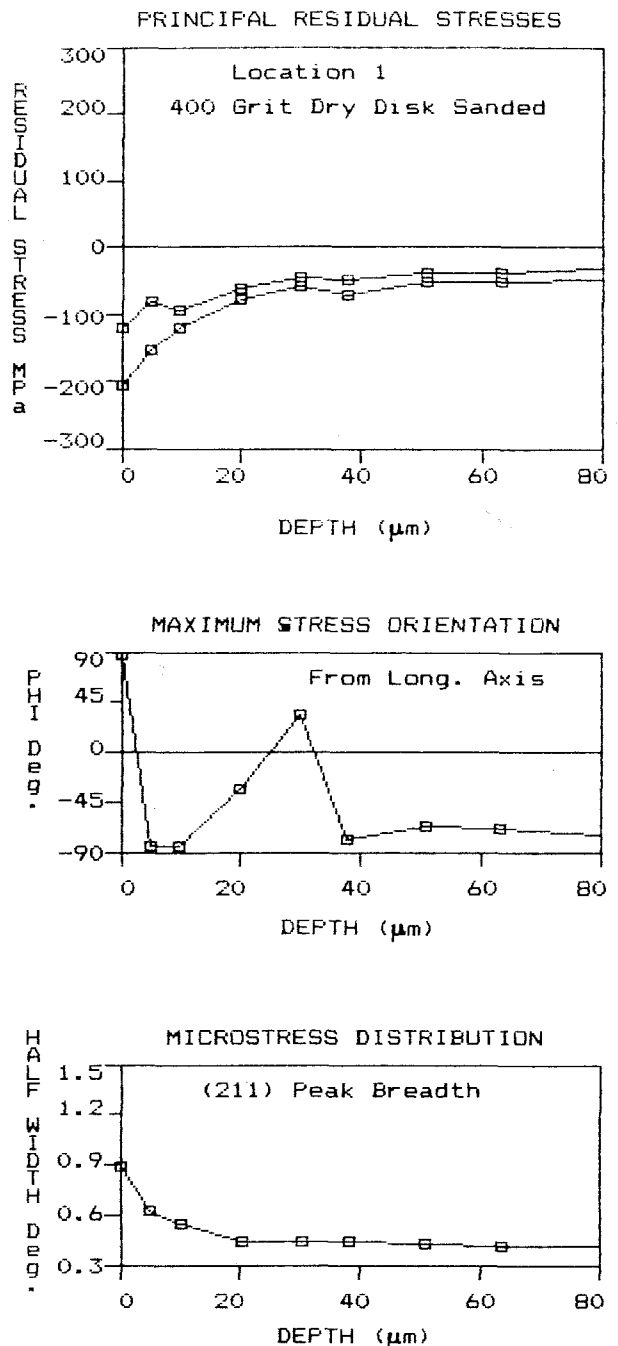

Fig. 2—Principal-residual-stress distributions produced by 400-grit dry-disk sanding

measured. Because the biaxial stress field is symmetrical, the degree of variation of ϕ with depth indicated by the linear interpolation may be exaggerated.

All of the abrasive surface-preparation methods which produce little or no heating of the surface, shown in Figs. 1-4, produced very similar macrostress and microstress distributions. The wet lapping methods, with no significant heat generation, produced the highest surface compression on the order of −250 MPa. The dry sanding produced lower magnitude surface compression, on the order of −200 MPa, with otherwise similar form. The microstress
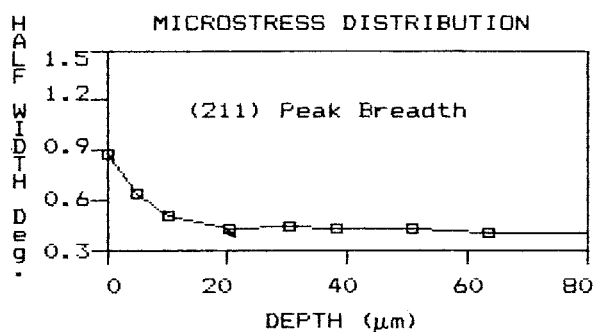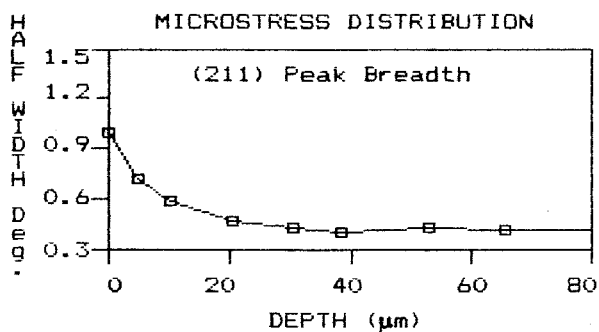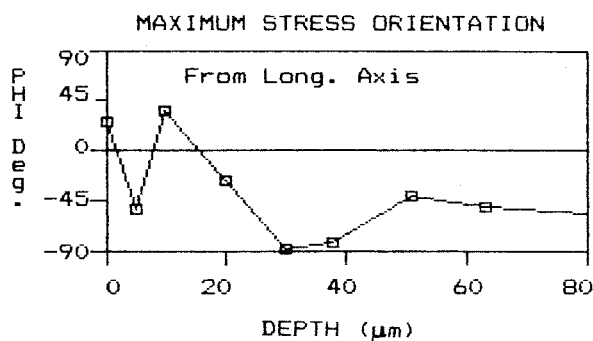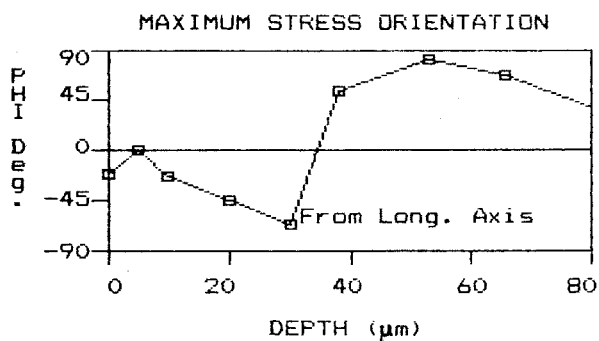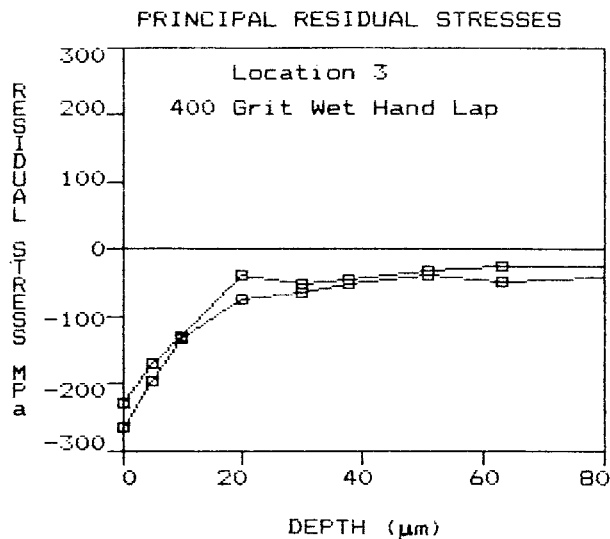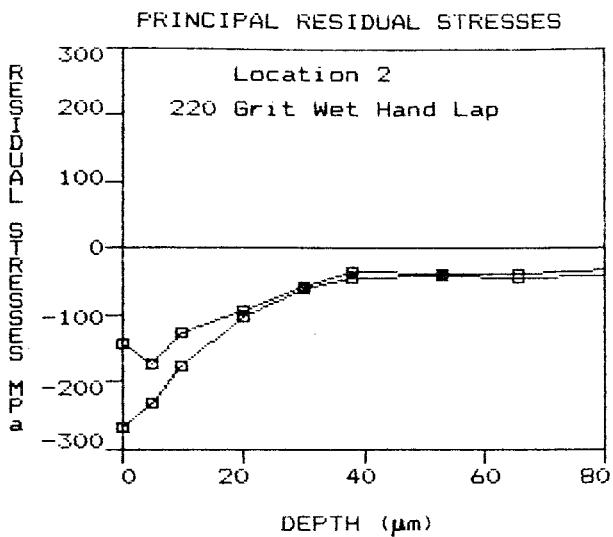
Fig. 3—Principal-residual-stress distributions produced by 220-grit wet hand lapping

Fig. 4—Principal-residual-stress distributions produced by 400-grit wet hand lapping

distributions indicate nearly identical magnitudes and depths of the deformed surface layer, extending to approximately 20 to 40 μm, with the coarser 220 grit producing the deeper deformed layer.

The effect of nital etching of the surface is shown in Fig. 5. The microstress results show no significant plastic deformation. Residual stresses do, however, appear to be induced by the etching process, perhaps associated with the formation of corrosion products. A maximum residual stress on the order of +40 MPa was induced at the surface, which diminished over a depth of approximately 10 μm.

The residual-stress distribution produced by dry power-belt sanding with 120-grit paper is shown in Fig. 6. The principal-residual-stress distributions were found to range from +200 MPa to −180 MPa at the surface, and to extend to a depth of 60 μm. The maximum stress direction is aligned near the direction of sanding to a depth of nominally 10 μm. Power sanding produced a cold-worked layer of approximately twice the depth and magnitude produced by other abrasive surface treatments.

Primary features of the stress distributions at the five locations are summarized in Table 2. The principal surface

PRINCIPAL RESIDUAL STRESSES

Location 4
Nital Etch

MAXIMUM STRESS ORIENTATION

From Long. Axis

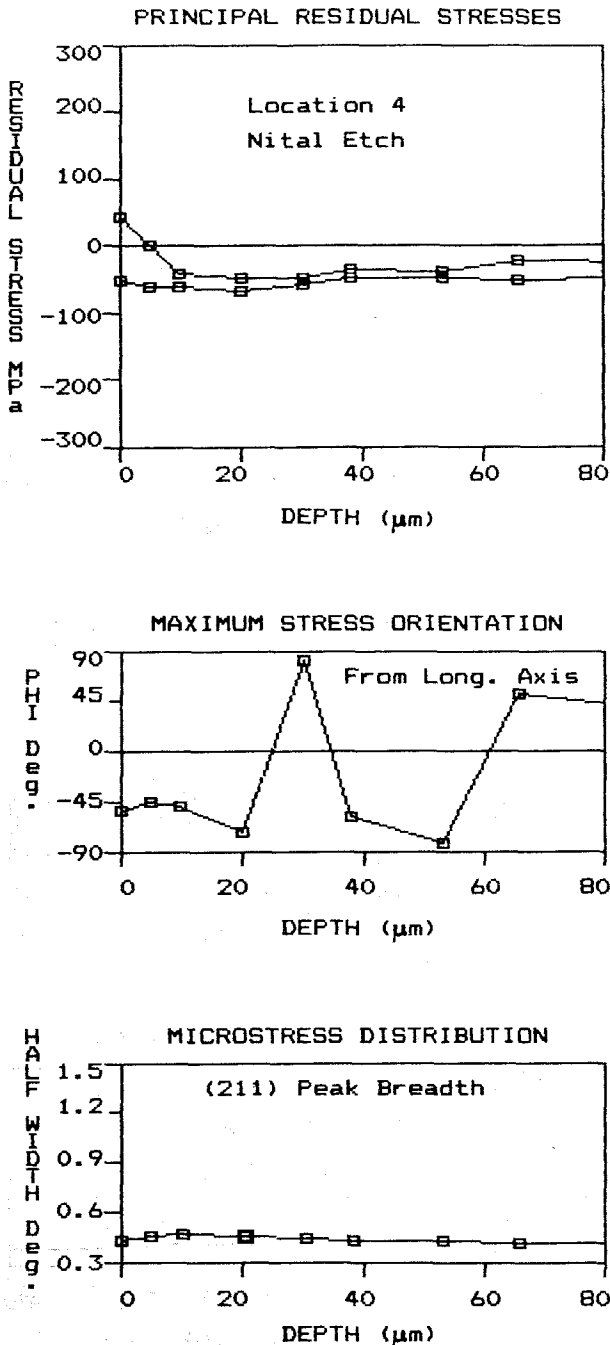## MICROSTRESS DISTRIBUTION

(211) Peak Breadth

Fig. 5—Principal-residual-stress distributions produced by nital etching

residual stresses are given with the orientation of the maximum stress relative to the transverse direction, which was the direction of abrasion. The microstress or degree of cold work is summarized in terms of the relative surface magnitude assuming that the subsurface (211) diffraction peak breadth of 0.43 deg represents fully annealed material, and arbitrarily assigning a magnitude of 1.0 to the peak breadth of 0.89 deg produced by 400-grit sanding. The nominal depth of both the macro and microstress distributions is shown.

The residual-stress distributions produced by the mechanical-abrasion surface-preparation methods may be understood in terms of a superposition of residual stresses produced by two processes: tensile deformation of the surface layers caused by the cutting action of the abrasive grit during polishing, and compressive deformation of the surface layers caused by thermal stresses developed in the confined surface layer due to heat generated by friction.

In the case of wet lapping, with no heat evolved, the highly compressive residual stresses result solely from tensile deformation during the cutting of the surface by the abrasive grit. During dry sanding, the surface in immediate contact with the abrasive may be heated to the point that the yield strength diminishes significantly. The heated confined surface layer yields in compression due to the constraint imposed by the cold subsurface material. Compressive yielding of the hot surface results in a tensile component of residual stress when the surface has cooled. Superposition of the thermal tensile stresses tends to cancel the compressive stresses due to cutting, resulting in reduced surface compression as in the case of the 400-grit dry disk sanding shown in Fig. 2. If the thermal component is of sufficient magnitude, tensile stresses are produced at or near the surface, as shown for the 120-grit dry belt sanding in Fig. 6.

Although the simple superposition of thermal and cutting stresses appears to account for the primary features of the residual-stress distributions observed, the process of surface abrasion is far more complex. Actual thermal and cutting stress distributions will generally be complex functions of directions and depth. Phase transformations, dependent upon the instantaneous temperatures and pressures developed, will contribute to the residual stresses produced in some materials.

All of the locations investigated showed low magnitude compressive residual stresses on the order of −40 MPa beneath the layer influenced by surface preparation. This confirms observations made during participation in the SEM round-robin study. The possibility of this stress being a result of systematic experimental error was eliminated by the use of a powdered-iron zero-stress standard, which showed a systematic additive error due to all forms of instrument misalignment and sample displacement of −2 MPa.

Elimination of systematic additive instrumental error, the adherence of the lattice strain to the plane-stress model assumed and the consistency with which the nominally −40 MPa subsurface stress was observed, support the conclusion that the body-centered-cubic ferritic phase in which strain measurements were made is in low magnitude compression, even after the extensive annealing treatment.

Conclusions

The results of this investigation to determine the residual-stress distributions induced by recommended strain-gage surface-preparation methods appear to support the following conclusions.

First, mechanical-abrasive techniques for surface preparation will induce residual stresses which could alter residual-stress distributions produced by machining, grinding or shot peening, which may be the subject of study. The macroscopic stress distributions produced by hand lapping will generally be compressive and of high magnitude approaching 80 percent of the yield strength of the material at the surface, and diminish nearly exponentially with depth to 30 μm. More aggressive surface treatments, such as belt sanding, may induce tensile stresses of comparable magnitude and extending to depths of 60 μm.
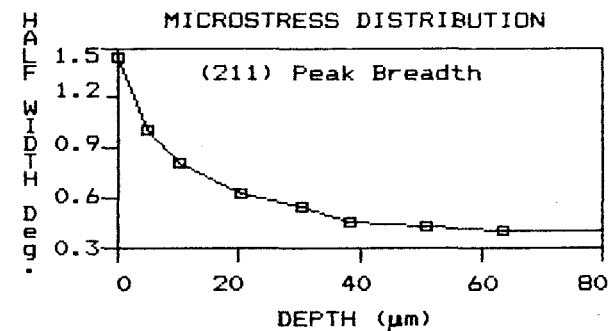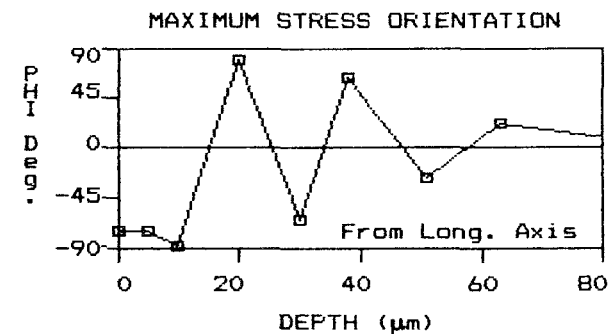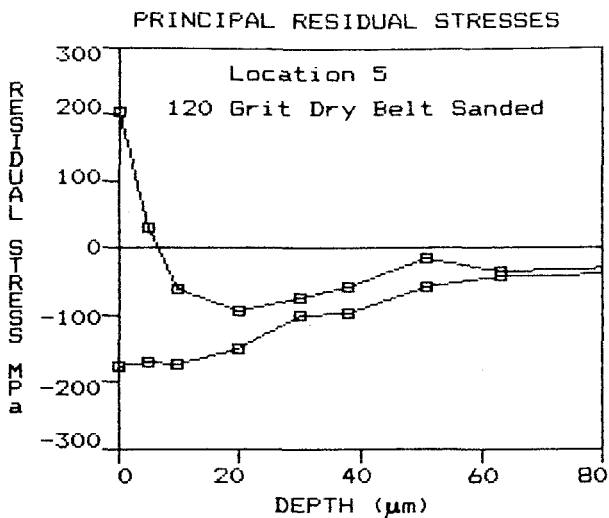
PRINCIPAL RESIDUAL STRESSES

Location 5
120 Grit Dry Belt Sanded

(graph: RESIDUAL STRESS MPa vs DEPTH (μm), vertical axis from -300 to 300, horizontal axis from 0 to 80)

MAXIMUM STRESS ORIENTATION

(graph: PHI Deg. vs DEPTH (μm), vertical axis from -90 to 90, horizontal axis from 0 to 80, labeled "From Long. Axis")

MICROSTRESS DISTRIBUTION

(211) Peak Breadth

(graph: HALF WIDTH Deg. vs DEPTH (μm), vertical axis from 0.3 to 1.5, horizontal axis from 0 to 80)

Fig. 6—Principal-residual-stress distributions produced by 120-grit dry-belt sanding

TABLE 2—SUMMARY OF RESIDUAL-STRESS DISTRIBUTIONS PRODUCED BY SURFACE PREPARATION OF 1018 STEEL

Surface Preparation	Surface Macro-stress (MPa)		Orientation (deg) (a)	Microstress Magnitude (b)	Depth (μm)
	Maximum	Minimum			
400-grit dry sanded	− 123.	− 206.	0-5	1.0	20
220-grit wet lap	− 143.	− 270.	70-90	1.3	40
400-grit wet lap	− 230.	− 265.	0-45	1.0	20
Nital Etch	+ 43.	− 54.	45	0.0	0
120-grit dry sanded	+ 202.	− 176.	0-15	2.3	60

(a) Angle from the maximum stress to the transverse direction.
(b) Relative magnitude assuming 400 grit = 1, fully annealed = 0.

some method of abrasive surface preparation for strain-gage application, the residual stresses induced were not detected. Therefore, residual stresses near the surface, even of high magnitude, were not resolved by full-depth hole drilling, and stresses induced in surface preparation could be ignored. If, however, the method is extended by incremental drilling to study the stresses near the surface of a sample, the residual stresses induced by surface preparation may need to be considered.

References

1. "Standard Method for Determining Residual Stresses by the Hole-Drilling Strain-Gage Method," Annual Book of ASTM Standards, ASTM, Philadelphia, 3.01 (E837), 782-787 (1984).
2. Niku-Lari, A., Lu, J. and Flavenot, J.F., "Measurement of Residual-Stress Distribution by the Incremental Hole-Drilling Method," EXPERIMENTAL MECHANICS, 25 (2), 175-185 (June 1985).
3. Flaman, M.T. and Manning, B.H., "Determination of Residual-Stress Variation with Depth by the Hole-Drilling Method," EXPERIMENTAL MECHANICS, 25 (3), 205-207 (Sept. 1985).
4. SEM Residual Stress Measurement Committee, "Bulk-Zero Stress Standard - AISI 1018 Carbon-Steel Specimens, Round Robin Phase I," secretary J.J. Yavelak, EXPERIMENTAL TECHNIQUES, 9 (4), 38-41 (April 1985).
5. Alloy Digest, AISI 1018 Steel Spec. Sheet CS-56, Eng. Alloy Dig. (March 1985).
6. "Residual Stress Measurement by X-Ray Diffraction," ed. M.E. Hilley, SAE J784a, Soc. Auto. Eng., Warrendale, PA, 19 (1971).
7. Prevey, P.S., "The Use of Pearson VII Distribution Functions in X-Ray Diffraction Residual Stress Measurement," Advances in X-Ray Analysis, Plenum Press, NY, 29, 103-112 (1986).
8. Prevey, P.S., "A Method of Determining the Elastic Properties of Alloys in Selected Crystallographic Directions for X-Ray Diffraction Residual Stress Measurement," Advances in X-Ray Analysis, Plenum Press, NY, 20, 345-354 (1977).
9. "Residual Stress Measurement by X-Ray Diffraction," ed. M.E. Hilley, S.A.E. J784a, Soc. Auto. Eng., Warrendale, PA 61 (1971).
10. Moore, M.C. and Evans, W.P., "Mathematical Corrections for Stress in Removed Layers in X-Ray Diffraction Residual Stress Analysis," SAE Trans., 66 (1958).
11. "Standard Method for Verifying the Alignment of X-Ray Diffraction Instrumentation for Residual Stress Measurement," Annual Book of ASTM Standards, ASTM, Philadelphia, PA, 3.01 (E915), 809-812 (1984).
12. Prevey, P.S., "Surface Residual Stress Distributions in As-Bent Inconel 600 U-Bend and Incoloy 800 90-Degree Bend Tubing Samples," Workshop Proc.: U-Bend Cracking in Steam Generators, Elec. Power Res. Inst., Palo Alto, CA, 12-3 to 12-19 (1981).
13. "Residual Stress Measurement by X-Ray Diffraction," ed. M.E. Hilley, SAE J784a, Soc. Auto. Eng., Warrendale, PA, 20 (1971).

Second, mechanical-surface-preparation methods induce a cold-worked layer, the magnitude and depth of which is a function of the severity of the mechanical treatment. Coarser grit and higher pressures produce greater magnitude and depth of the deformed layer. The depth of the deformed layer extends to approximately the depth of the macroscopic-residual-stress field induced. Etching of the surface appears to induce no significant plastic deformation, and only slight surface macroscopic stresses.

The results of the SEM round robin[4] demonstrate that, although virtually all the hole-drilling participants used